PHYSICAL REVIEW B **81**, 121101(R) (2010)

Strong optomechanical interaction in a bilayer photonic crystal

Young-Geun Roh,[1,2,*] Takasumi Tanabe,[1,2] Akihiko Shinya,[1,2] Hideaki Taniyama,[1,2] Eiichi Kuramochi,[1,2] Shinji Matsuo,[3] Tomonari Sato,[3] and Masaya Notomi[1,2,†]

[1]*NTT Basic Research Laboratories, NTT Corporation, 3-1 Morinosato-Wakamiya, Atsugi, 243-0198, Japan*

[2]*CREST-JST, 4-1-8, Honmachi, Kawaguchi, Saitama 332-0012, Japan*

[3]*NTT Photonics Laboratories, NTT Corporation, 3-1 Morinosato-Wakamiya, Atsugi, 243-0198, Japan*

(Received 10 December 2009; published 9 March 2010)

We fabricated bilayer photonic crystal (PhC) as large as 20×30 μm possessing 200-nm-thick slabs and a 200-nm-thick air gap. Input power dependence of reflectance spectra indicates air gap reduction by 3.6 nm. Combining it with finite element method calculation we estimate optomechanically generated force per unit stored energy as 0.4 μN/pJ, exhibiting strong optomechanical coupling. RF spectrum of reflected light reveals intensity modulation by thermal vibration of bilayer PhC, which also shows strong interaction of optical resonance mode and mechanical mode of bilayer PhC

DOI: 10.1103/PhysRevB.81.121101 PACS number(s): 42.70.Qs, 43.40.Dx, 05.40.Jc

Optomechanical interaction based on the radiation force has been studied for over a century since Maxwells pioneering work,[1] which has been applied in various phenomena ranging from optical tweezers,[2] optical microelectromechanical system (MEMS),[3] and laser cooling of macroscale mirrors.[4] In general, optomechanical coupling between light and matter is insignificant since a photon does not have rest mass, but its effect can be enhanced for a structure with small mass and strong light confinement. Indeed, recent progress in miniaturized photonic structures such as microring cavities[5] or toroidal cavities[6] has enabled successful observation of various interesting phenomena, such as laser cooling of micromirrors/microcavities[7] and optically driven mechanical oscillation via radiation pressure.[8,9]

In order to enjoy larger optomechanical coupling, we should employ smaller and higher-Q cavities with appropriate mechanical degree of freedom. In terms of this issue, optical cavities based on photonic crystals (PhCs) are apparently advantageous since ultrahigh-Q and wavelength-sized cavities [$Q>10^6$ and $V_{eff}\sim(\lambda/n)^3$, where V_{eff} is the cavity mode volume] have been demonstrated only in them.[10,11] From this background, we proposed bilayer PhC slab structures [shown in Fig. 1(a)] in 2006.[12] This bilayer PhCs can maintain various superior features of conventional single-layer PhC slabs such as ultrahigh-Q with small V_{eff}. In the previous paper, we showed that this configuration leads to enormously large optomechanical coupling since we can introduce the mechanical displacement in the vicinity of the intensity peak of the microcavity mode. Recently, similar bilayer cavity systems based on microring cavities have been reported,[13,14] but the fabrication of bilayer PhCs has not been reported yet. In this Rapid Communication, we report successful realization of bilayer PhC slabs and observation of mechanical displacement due to strong radiation force generated by band-edge modes,[15] which demonstrates large optomechanical coupling in bilayer PhCs.

Here we employ simple structures fully clamped 2D PhC membranes shown in Fig. 1(a). The optical resonant modes interested are based on band-edge modes in PhCs. This configuration allows us to input/output light in the vertical direction very efficiently without implementing waveguides. We can expect large $F=-dU/dz$, general form of exerted radiation force ($U=N\hbar\omega_c$ is stored energy inside cavities and z is spatial coordinate of vertical direction) because $d\omega_c/dz$ for band-edge modes is mostly the same as that for defect modes. Although we cannot expect ultrahigh-Q nor ultrasmall V_{eff} for band-edge mode, we regard it is an important feature to demonstrate the large optomechanical interaction based on $F=-dU/dz$ in the bilayer PhCs. In addition, the use of the band-edge mode is practically very effective to generate strong radiation force because one can easily couple an intense light beam without causing significant optical nonlinear absorption.

In this work, bilayer PhCs were fabricated from an InP (200-nm-thick)/InGaAs (200 nm)/InP (200 nm)/InGaAs (1000 nm) multilayer. Two InP layers serve as PhC slabs, and the other two InGaAs layers are used as sacrificial layers. A periodic hole pattern arranged in a square lattice was defined

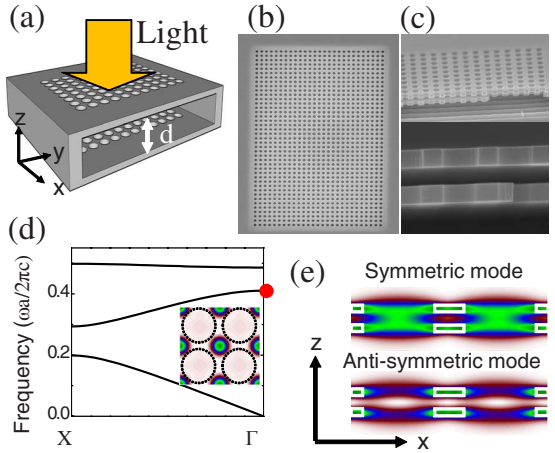

FIG. 1. (Color online) (a) Schematics of experiment. The structure is fully clamped (all-side clamped) (b) Top-view scanning electron microscope image, (c) Bird's-eye view (upper) and cross section (lower) of bilayer PhC. Period is 750 nm and hole radius at the center is 270 nm. (d) 2D photonic band structure of TE mode with $n=2.8$ (effective index for TE mode). Inset is the lateral plot of $|Hz|^2$ at the Γ point indicated by red dot (e) Vertical mode profiles of $|Hz|^2$ in the double slab at the Γ point indicated in (d).

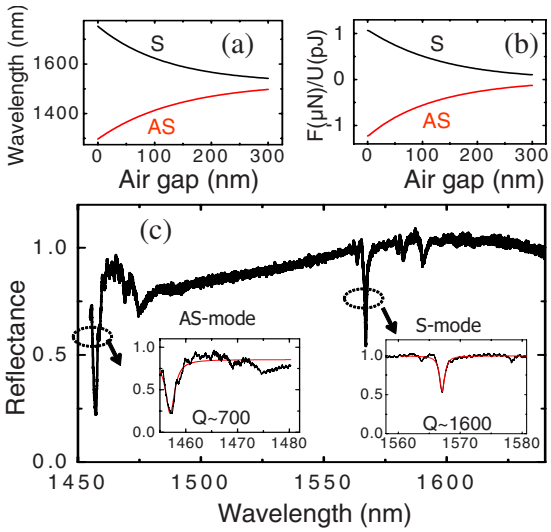

FIG. 2. (Color online) (a) Resonant wavelength of band-edge modes as a function of air gap width. Band-edge modes for the lattice constant of 750 nm hole radius of 270 nm were calculated using plane-wave expansion method and exponentially fitted. (b) force per unit stored energy as a function of air gap width. Positive value means attractive one. (c) Reflectance spectrum of the bilayer PhC with 20×30 μm. Insets show the zoom-in of each resonance curve and fitted to Lorentzian.

using e-beam lithography. Cl_2-based ICP etching is used to transfer the pattern into the InP/InGaAs multilayer system. The InGaAs layers were selectively etched by citric acid.[16] We employed CO_2 supercritical drying method[17] to prevent stiction as a result of the capillary force. All sides of the bilayer PhC were fully clamped. By adopting these procedures, we successfully fabricated bilayer InP PhC slabs as shown in Figs. 1(b) and 1(c) which are scanning electron microscope images of a 20×30 μm bilayer square air-hole PhC with the lattice constant of 750 nm and air gap of 200 nm. In this sample, the hole radius was gradually modulated from 270 nm at the center to 200 nm at the edge. This modulation makes the band-edge modes loosely confined with the full width at half maximum of 3.0 μm, which was approximately matched with the input light beam width. Although in-plane standing-wave modes are formed by the modulation, the optomechanical response can be explained with a simple band-edge mode described in the Figs. 1(d) and 1(e) due to its weak confinement. We confirmed that the modulation does not alter essential properties except the coupling efficiency with the input beam.

We adopted a band-edge mode at the Γ point often used in vertical emitting lasers [red dot in Fig. 1(d)], a well-known high-Q mode owing to its in-plane symmetry as well as low group velocity.[18,19] In our bilayer systems, the band-edge modes in two slabs are coupled each other to form two coupled modes with even and odd symmetry with respect to the vertical direction. Figure 1(e) shows intensity profile of symmetric (hereafter we denote this as the S) and antisymmetric (AS) modes in bilayer PhCs. Figure 2(a) shows two coupled modes as a function of the air gap width calculated by the plane-wave expansion method. Similar to our previous studies,[12] coupled modes in bilayer PhCs exhibit strong

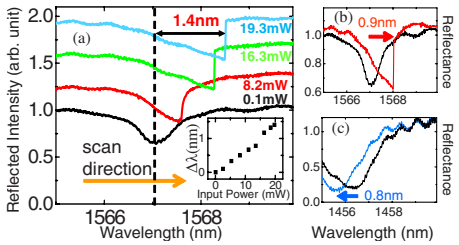

FIG. 3. (Color online) (a) Reflectance obtained by wavelength scanning with varying the input power. Dotted line indicates the initial resonance position $\lambda=1567.1$ nm Wavelength scan is always done from short to long wavelength. Resonance shift is defined from initial wavelength to the abrupt kink on the spectra. Inset shows the linearity between input power and redshift of resonance. (b) Reflectance spectra by wavelength sweeping across S-mode and (c) AS mode. In (b), input powers were 0.1 mW (thick black curve) and 13 mW (thin red curve). (c) was taken with low power (thick black curve) while irradiating cw pump beam at $\lambda=1568.0$ nm with input power of 13 mW (thin blue curve)

dependence on the gap width because two slab modes are strongly coupled via a small air gap. The radiation force per unit electromagnetic energy in the cavity can be calculated by $F/U=-1/\omega(d\omega/dz)$. The force calculated from Fig. 2(a) is plotted in Fig. 2(b), which shows that considerably large force can be generated in this cavity. For convenience, we take the positive sign as the attractive force. Note that the S mode exerts an attractive force while the AS mode exerts a repulsive force.

To characterize the resonant modes in the fabricated bilayer PhC sample, we adopted the reflectance spectrum measurement. A light beam from a tunable laser was focused vertically onto the sample in air using an objective lens with a numerical aperture (NA) of 0.42. The beam diameter was estimated to be about 2 μm. Polarization direction of the light is parallel to the one of the axes of the square lattice of the bilayer PhC. In Fig. 2(c), we plot the reflectance spectrum obtained with a small input power of 32 nW. There are two distinctive dips in the spectrum at around 1567.1 and 1457 nm, which clearly indicate resonant features. The measured Q factors for these resonances are 1600 and 700, respectively. The measured wavelengths agree very well with the calculated values for the S mode with $\lambda=1559$ nm and for the AS mode with $\lambda=1463$ nm, respectively, in Fig. 2(a). To examine the effect from the radiation force on our sample, we investigated the input power dependence of the reflectance spectra around the S mode, as shown in Fig. 3(a). The spectra were measured by sweeping the wavelength of the incident laser across the S mode ($\lambda=1567.1$ nm) at various input power from 0.1 to 19.7 mW. In Fig. 3(a), we can see a clear redshift in the resonance dip as the input power increases. With an input power of 19.7 mW, the resonance mode, which was initially at $\lambda=1567.1$ nm, is redshifted by 1.4 nm. This result agrees very well with our expectation of generating attractive force and decreasing air gap when S mode is excited The corresponding change in the air gap is estimated to be $\Delta d=-4$ nm from Fig. 2(b). The cusplike spectral shapes are due to the occurrence of optical bistability,[20] which is a direct consequence of the fact that the

resonant wavelength depends on the input power. Similar bistability has been observed in other optomechanical systems.[13,21] The result in Fig. 3(a) strongly suggests the optically induced displacement, but we need to check the thermal contribution because the thermal heating also causes redshift.[22] Linearity of wavelength shift in the inset of Fig. 3(a) excludes the nonlinear heating process such as two photon absorption (primary heating process in InP). Hence the thermal effect may not be the cause of the redshift. To more directly confirm whether the spectral shift is caused by the mechanical or thermal effects, we performed another experiment which distinguishes the shift orientation according to the symmetry of two modes. First, we measured the reflectance spectrum around the *S* mode with substantially intense pumping power at 13 mW and obtained the reflectance spectrum seen in Fig. 3(b) which results in a resonance shift of $\Delta\lambda=+0.9$ nm. Next, we measured the reflectance spectrum of the AS mode with a weak probe light while strongly pumping the *S* mode simultaneously. The *S* mode pumping is done by a laser fixed at $\lambda=1567.95$ nm which is just 0.05 nm shorter than a bistability kink in Fig. 3(b). This cw pumping fixes the system so that it is detuned by $\Delta\lambda=+0.9$ nm with respect to the *S* mode. Simultaneously we measured the reflectance spectrum around the AS mode with a low input power. We show the result in Fig. 3(c), which exhibits a clear blueshift in the resonance of as large as 0.8 nm. This result cannot be explained by the thermo-optic effect which only causes redshift, and well explained by the mechanical movement of slabs.

To examine the contribution more in detail, we quantitatively compare it with theoretical estimation. From the result in Fig. 2(b), we can estimate the blueshift to redshift ratio for two modes to be $|\Delta\lambda_{blue}/\Delta\lambda_{red}|=1.09$. This value is slightly larger than the experimental value of 0.8 nm/0.9 nm=0.89. Thus, this small derivation might be due to the thermo-optic effect. The corresponding temperature increase ΔT is maximally 3 K at the condition in Figs. 3(b) and 3(c). Using this result, we can derive that 90.7% (1.27 nm) of the observed redshift is due to the slab displacement. From the result of the photonic band calculation [Fig. 2(b)], the corresponding gap change is $\Delta d=-3.6$ nm. In this case the thermomechanical effect due to the thermal-expansion results in less than 30 p.m. deflection of slab. Thus, we can conclude that we successfully displaced the gap by 3.6 nm with radiation force as a result of optical pumping with 13 mW in our bilayer PhC systems.

Next, we estimate the force generated in our experiment and discuss the strength of optomechanical coupling in the bilayer PhCs. The finite element method (FEM) calculation shows that each PhC slab has a spring constant of 6.1 N/m. From the deduced gap change, the force is calculated to be 10.8 nN at 13 mW input. By taking the *Q* value of the *S* mode ($Q\sim1600$), the electromagnetic energy stored in the *S* mode is roughly 27 fJ. With these values, the minimum F/U value is determined as 0.4 μN/pJ. We regard this value is consistent with the theoretical value (0.23 μN/pJ) within measurement errors. The reason of the slight discrepancy might be due to inaccuracy in estimating the actual air gap width. We observed that the air gap width varies sample to sample by 50 nm probably due to the residual strain. Thus,

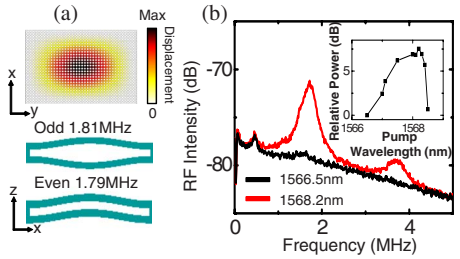

FIG. 4. (Color online) (a) Fundamental vibration modes with even ($f=1.79$ MHz) and odd parity ($f=1.81$ MHz). (b) Radio frequency (RF) spectra of reflected light at $\lambda=1566.5$ nm (thick black curve) and $\lambda=1568.2$ nm (thin red curve). (c) Relative peak power in RF spectrum as a function of wavelength. Reference value was taken to the peak power at $\lambda=1566.5$ nm.

we can safely conclude that strong optomechanical interaction in bilayer configuration has been confirmed in our bilayer PhCs. Note that our F/U value is similar to the values for double-layer disk cavities[13,14] and for zipper cavities[23,24] with the similar gap size, but it is 1 order of magnitude larger than conventional optomechanical systems such as toroidal cavity,[25] that is, systems other than bilayer systems or their equivalent. Hence, advantage of bilayer systems against conventional one-layer systems has been clearly demonstrated in two-dimensional (2D) photonic crystals in our experiments.

Thus far, we have investigated optomechanical coupling between optical resonant modes and mechanical displacement. In many applications including back-action laser cooling and optically driven vibration, however, it is important to realize optomechanical coupling between optical resonant modes and mechanical resonant modes. A vibration analysis using FEM reveals that our bilayer PhC membrane has well-defined even and odd fundamental vibrating modes around $f_0=1.79$ and 1.81 MHz as shown in Fig. 4(a). Since the radiation force should drive odd vibrating mode (two modes in each slab vibrate in opposite phase), there would be efficient coupling between the optical mode and this odd vibrating mode.

To directly observe this phenomenon, we analyzed the reflected power in the frequency domain using a RF spectrometer with constant optical pumping of 19.7 mW. Figure 4(b) shows the RF spectrum of a reflected signal with pumped at $\lambda=1568.2$ and 1566.5 nm. At the pumping wavelength far from the optical resonance, there is no significant peak, but when pumped in the vicinity of the resonance, distinctive peaks appear. The frequency of the first peak is 1.8 MHz, which is reasonably close to the fundamental vibrating mode found in the FEM calculation. The RF peak intensity is plotted as a function of the pumping wavelength in the inset of Fig. 4(b). The peak is maximum at $\lambda=1568.2$ nm. corresponding to the "steepest" point of the Lorentzian line shape with resonance at $\lambda=1568.5$ nm and 1 nm linewidth obtained in experiment. Since the RF intensity should be proportional to the derivative of the reflectance spectrum, this correspondence is reasonable and indicates that the optical reflected signal from the optical resonance mode is indeed modulated by the mechanical resonant mode. We regard that the other RF peak at $f=3.7$ MHz is a second harmonic of $f_0=1.8$ MHz, resulting from the nonlinear

transfer function between the optical mode and mechanical mode.[26]

Low mechanical $Q \sim 2$ (limited by air damping) implies that the peak is due to the Brownian vibration, not a forced one. The amplitude of the thermal Brownian vibration is roughly estimated to be $(k_B T/k)^{1/2}=30$ pm where k_B is the Boltzmann constant and the spring constant $k=6.1$ N/m, and $T=300$ K. We confirmed that the amplitude of the optical output intensity is consistent with this amplitude of Brownian vibration. In spite of the very low Q value we can observe such a tiny motion in our bilayer structure thanks to the strong optomechanical coupling.

In conclusion, we successfully fabricated bilayer PhCs and observed large optomechanical coupling by employing band-edge modes. Furthermore, efficient coupling between optical modes and mechanical modes was confirmed by the observation of Brownian modes in the RF signal of the reflected light. Our result clearly showed that bilayer PhCs can serve strongly coupled optomechanical systems. We believe that 2D bilayer PhCs have high potential as optomechanical systems in terms of strong light confinement because 2D PhCs can serve ultrahigh-Q performance as have already reported. A combination of the present study with ultrahigh-Q beam cavities in 2D photonic crystal[27] would be ideal for such purpose. Actuation using the band-edge mode employed in this study is also promising for application as a MEMS actuator because it can generate a gigantic radiation force as we mentioned before.

*ygroh@nttbrl.jp
†notomi@nttbrl.jp

[1] J. C. Maxwell, *A Treatise on Electricity and Magnetism* (Clarendon, Oxford, 1874), Vol. 2, p. 792.
[2] A. Ashkin, Phys. Rev. Lett. **24**, 156 (1970).
[3] J. E. Graebner, S. Pau, and P. L. Gammel, Appl. Phys. Lett. **81**, 3531 (2002).
[4] D. Reitze, Nat. Photonics **2**, 582 (2008).
[5] A. Gondarenko, J. S. Levy, and M. Lipson, Opt. Express **17**, 11366 (2009).
[6] D. K. Armani, T. J. Kippenberg, S. M. Spillane, and K. J. Vahala, Nature (London) **421**, 925 (2003).
[7] S. Gigan, H. R. Bohm, M. Paternostro, F. Blaser, G. Langer, J. B. Hertzberg, K. C. Schwab, D. Bauerle, M. Aspelmeyer, and A. Zeilinger, Nature (London) **444**, 67 (2006).
[8] T. J. Kippenberg, H. Rokhsari, T. Carmon, A. Scherer, and K. J. Vahala, Phys. Rev. Lett. **95**, 033901 (2005).
[9] T. Carmon, H. Rokhsari, L. Yang, T. J. Kippenberg, and K. J. Vahala, Phys. Rev. Lett. **94**, 223902 (2005).
[10] Y. Akahane, T. Asano, B.-S. Song, and S. Noda, Nature (London) **425**, 944 (2003).
[11] E. Kuramochi, M. Notomi, S. Mitsugi, A. Shinya, T. Tanabe, and T. Watanabe, Appl. Phys. Lett. **88**, 041112 (2006).
[12] M. Notomi, H. Taniyama, S. Mitsugi, and E. Kuramochi, Phys. Rev. Lett. **97**, 023903 (2006).
[13] J. Rosenberg, Q. Lin, and O. Painter, Nat. Photonics **3**, 478 (2009).
[14] Q. Lin, J. Rosenberg, X. Jiang, K. J. Vahala, and O. Painter, Phys. Rev. Lett. **103**, 103601 (2009).
[15] V. Liu, M. Povinelli, and S. Fan, Opt. Express **17**, 21897 (2009).
[16] G. C. DeSalvo, W. F. Tseng, and J. Comas, J. Electrochem. Soc. **139**, 831 (1992).
[17] H. Namatsu, J. Vac. Sci. Technol. B **18**, 3308 (2000).
[18] K. Sakoda, *Optical Properties of Photonic Crystals*, 2nd ed. (Springer-Verlag, Berlin, 2004).
[19] M. Imada, S. Noda, A. Chutinan, T. Tokuda, M. Murata, and G. Sasaki, Appl. Phys. Lett. **75**, 316 (1999).
[20] T. Carmon, L. Yang, and K. Vahala, Opt. Express **12**, 4742 (2004).
[21] M. Eichenfield, C. P. Michael, R. Perahia, and O. Painter, Nat. Photonics **1**, 416 (2007).
[22] V. S. Ilchenko and M. L. Gorodetskii, Laser Phys. **2**, 1004 (1992).
[23] M. Eichenfield, R. Camacho, J. Chan, K. J. Vahala, and O. Painter, Nature (London) **459**, 550 (2009).
[24] R. M. Camacho, J. Chan, M. Eichenfield, and O. Painter, Opt. Express **17**, 15726 (2009).
[25] A. Schliesser, O. Arcizet, R. Riviere, G. Anetsberger, and T. J. Kippenberg, Nat. Phys. **5**, 509 (2009).
[26] T. Carmon and K. J. Vahala, Phys. Rev. Lett. **98**, 123901 (2007).
[27] E. Kuramochi, H. Taniyama, T. Tanabe, A. Shinya, and M. Notomi, Appl. Phys. Lett. **93**, 111112 (2008).